Effect of Environmental Factors on the Mechanical Properties of Grafted Casein Films: Influence of Humidity and Biaxial Orientation

N. SOMANATHAN

Polymer Laboratory, Central Leather Research Institute, Adyar, Madras 600 020, India

SYNOPSIS

Casein was grafted with acrylonitrile and with a binary mixture of acrylonitrile and *n*-butyl methacrylate. The influence of absorbed moisture at different relative humidities on the stress–strain characteristics was studied. Tensile properties were very much affected by the absorbed moisture in both cases. The effect produced by water was very much pronounced in the case of casein grafted with acrylonitrile. Although the absorbed moisture level was the same in both grafted caseins, due to the influence of *n*-butyl methacrylate chains, which reduces the T_g of the film, the tensile properties and fracture behavior were very different from the films of casein grafted with acrylonitrile. Due to the application of stress in the lateral direction, tensile strength and elongation at break in the longitudinal direction was reduced. Both systems show that after an applied lateral stress of 5×10^{-2} Mpa the variation of stress and strain was not characteristic and the value levels off after that level. © 1996 John Wiley & Sons, Inc.

INTRODUCTION

The problems in casein films which are used as a leather coating, viz., hydrophilicity and brittleness, can be modified by grafting casein with suitable monomers. Like other biopolymers[1-6] casein[7-10] is also grafted with various monomers in order to make it suitable for application. The literature[11] suggests that acrylonitrile (AN) grafting is advantageous when compared to other acrylic monomers.

The literature on casein grafting shows that little attention has been paid to the properties under processing and end-use conditions. The physical properties[12] of the polymers are governed by several variables such as temperature, rate of straining, and plasticization.

Plasticization is a process of the addition of a relatively low molecular weight substance to a polymer to increase its flow properties. Plasticization[13,14] can be classified into two types, viz., internal and external plasticization. The absorbed water in the polymer can act like a plasticizer and can alter the properties of the polymer to a considerable extent.[15-20] Any process affecting the amorphous phase will exert a corresponding effect on the glass transition temperature. This is true for hydrophillic polymers where the decrease in the glass transition temperature due to plasticization affects the mechanical properties.

The effect of absorbed water on the properties of polymers was studied by many workers.[21,22] In the case of polyamides,[23,24] the absorbed moisture affects the mechanical properties and the failure mechanisms were also modified by the level of water present in these systems.

The presence of functional[25] groups in a polymer determines the various types of interactions such as hydrophillic, van der Waals, and electrostatic. When the plasticizer is incorporated into the polymer matrix, it interposes itself between the polymer chains.

Casein, being a glycoprotein, is hydrophilic in nature. Grafting of casein brings out modification in the structure, which, in turn, affects the hydrophillic character and plasticizing effect of water. Therefore, it is necessary to study the effect of moisture on the mechanical properties of grafted casein films.

Journal of Applied Polymer Science, Vol. 62, 1407–1414 (1996)
 CCC 0021-8995/96/091407-08

Casein films are tested for their mechanical properties by stretching the films in one direction. Generally, these films, when tested in uniaxial tension, contract laterally in the transversal direction.[26] In practice, the finished films that are applied on leather are ordinarily subjected to forces in more than one direction simultaneously. Therefore, biaxial testing was done to obtain an idea of the realistic behavior of the films. This becomes more important in the case of shrinkable films.[27]

In most cases, a polymer behaves in a more brittle manner when subjected to biaxial stress than to uniaxial stress.[28–30] During biaxial stretching, the orientation of the material takes place in the sample.[31–36] In this present study, the effect of relative humidity and biaxial testing on the stress–strain behavior of grafted caseins was studied in detail.

EXPERIMENTAL

Grafting

Casein was grafted with 2 mol of an AN monomer at 60°C, using potassium persulfate (9.7×10^{-3} mol L^{-1}). In another set of experiments, casein was grafted with a binary mixture of (0.9 and 0.1 mol) AN and *n*-butyl methacrylate (*n*BMA) monomers. The procedure followed for grafting was discussed in our earlier publication.[37] The reaction was performed for 3 h at 60°C under a nitrogen atmosphere.

Film Formation

The reaction mixture obtained after the reaction was made into films over a Hg surface. The concentration of the graft copolymer corresponded to a 15% solid content on drying. The films were cast at 65% RH. The film thus obtained was removed from the Hg bed, dried in vacuum, and conditioned for 7 days at 65% RH in a desiccator. The thickness of the specimen was measured using a thickness gauge having a sensitivity of the order of 0.00025 cm. The thickness of the films used for the study was 50–100 μm. Tensile testing of the films was done using an Instron universal tensile tester (Model 1112).

Tensile Testing at Different Relative Humidities

For the humidity studies, the dumbbell-shaped specimens were kept in a desiccator containing a saturated solution of different salts[38] to condition the films at the required humidity for 7 days at 25°C. After 7 days, the stress–strain characteristics were measured at 25°C. A simple procedure used to test these samples was as follows: The samples were immediately wrapped in polyethylene sheets and the gripping area was left uncovered. Eight to ten samples were tested at different humidity levels in an Instron tester and the experiments were performed quickly to prevent any alteration in the testing condition of the RH. Care was taken to see that the externally covered polyethylene did not interfere in the mechanical testing other than to maintain the specimen in the testing humidity condition.

Biaxial Testing

For biaxial testing,[39,40] samples of the type shown in Figure 1 was used. The details of biaxial testing was discussed in our earlier publication.[39,40] The samples were conditioned at 65% RH at 25°C for 3 days. The samples were clamped with a pneumatic type of clamp in the longitudinal direction and clamped with mechanical clamping in the lateral direction. The load on the lateral direction was applied through the pulleys using inelastic thread and a pan as shown in Figure 1. The load was suspended in the lateral direction (i.e., perpendicular to the longitudinal axis) and the stress–strain characteristics in the longitudinal axis were studied. The stress in the lateral direction was varied from 0.5 to 45×10^{-2} MPa and four samples were tested for each set of experiments. The static load on the lateral direction

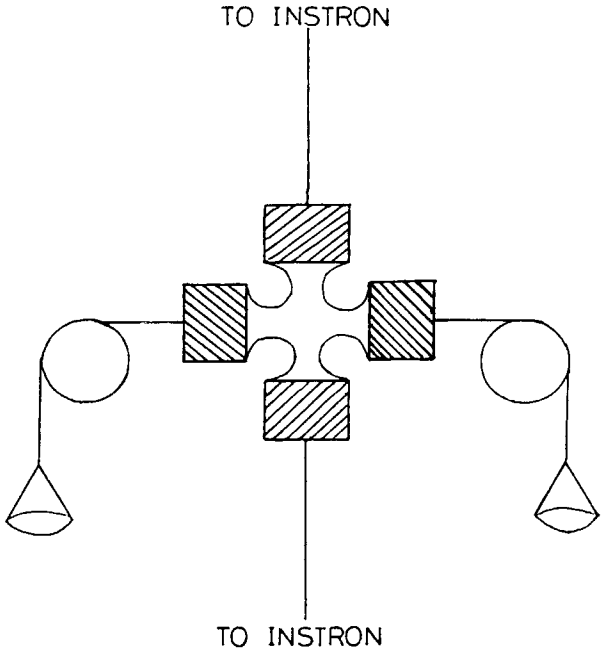

Figure 1 Biaxial testing attachment.

was applied instantaneously and, immediately, the sample was tested longitudinally with a strain rate of 0.5/min. The rate of straining in the lateral direction was varied, since the applied stress in the lateral direction was also varied. The creep effect produced by the lateral load was not worked out in this investigation. Biaxial testing was done at 25°C and 65% RH.

Moisture Sorption Studies

With P_2O_5 and various other salt solutions,[38] desiccators were kept at 0 and 95% RH. Films of grafted caseins were placed in small weighing bottles and conditioned at 0% RH. After 48 h, the weight of the bottle with the film was quickly determined to avoid external moisture condensation. The experiment was repeated until two consecutive readings did not vary by more than 1%. Following the same procedure, the weight of the film was determined at different RH. The weight at 0% RH was taken as the dry weight of the film.

RESULTS AND DISCUSSION

Effect of Relative Humidity

Moisture uptake of acrylonitrile-grafted casein (Ca-*g*-AN) and a binary mixture of grafted casein films (Ca-*g*-AN-*co*-*n*BMA) were studied at different RH levels and the results are presented in Table I. The moisture uptake gradually increases with increase of RH, and after 67% RH, the level of moisture rapidly increases in both cases. To understand the effect of grafting, the moisture absorbed by pure casein film at various RH is also presented in Table I. Table I shows that grafting tremendously reduces the absorbed moisture level, which suggests that polar sites were considerably reduced due to grafting.

Kulasekaran et al.[41] reported that during acrylonitrile grafting of casein amino acids like arginine, cystine, glycine, lysine, serine, threonine, and valine were the possible sites of the reaction. Infrared studies of grafted casein also show the variation of aromatic amino acid contents due to grafting.[42]

Comparison of the moisture sorption level of Ca-*g*-AN and Ca-*g*-AN-*co*-*n*BMA does not show any characteristic variation in the sorption level. These results suggest that the added *n*BMA chains do not characteristically change the moisture sorption level of AN-grafted casein.

The sorption characteristics were drawn and the thermodynamical parameters such as surface area and heat of sorption were calculated by applying the BET theory.[43] The BET equation, when monolayer coverage is complete, is given by

$$\frac{P/P_0}{V(1-P/P_0)} = \frac{1}{V_mC} + \frac{(C-1)P/P_0}{V_mC}$$

where P/P_0 = relative humidity, V = amount of moisture sorbed at a given RH, V_m = amount of water sorbed at monolayer coverage, and C = constant related to the net heat of sorption.

By plotting $(P/P_0)/V(1-P/P_0)$ against P/P_0, a straight line is obtained, and from the slope (S) and intercept (I), parameters such as heat of sorption and surface area can be calculated. The $\mathbf{R}^2$ values obtained for the straight-line fit for pure casein, Ca-*g*-AN and Ca-*g*-AN-*co*-*n*BMA are 0.943, 0.967, and 0.818, respectively:

$$V_m = 1/S + I$$

and

$$C = 1 + S/I$$

Knowing V_m and C, the surface area and heat of sorption can be calculated as

$$\text{Surface area} = 3431\ V_m\ \text{m}^2/\text{g}$$

$$\text{Heat of sorption} = RT \log_e C$$

where R is the universal gas constant, and T, the absolute temperature. Surface area, heat of sorption, etc., for grafted caseins are presented in Table II.

The amount of moisture sorbed at the monolayer coverage (V_m) increases with grafting. The same trend is also followed in the case of the surface area, whereas the heat of sorption decreases with grafting. Due to the incorporation of *n*BMA, the surface area increases further and the heat of sorption decreases further. With the incorporation of synthetic poly-

Table I Moisture Sorption of Grafted Casein at Different Relative Humidities (%)

RH	Pure Casein	Ca-*g*-AN	Ca-*g*-AN-*co*-*n*BMA
17	1.43	0.49	0.23
37	5.81	3.25	2.81
50	7.35	4.87	4.77
67	8.82	6.74	6.81
73	18.30	15.57	15.40
95	137.40	70.70	73.82

Table II Parameters Calculated Using BET Equation

	V_m	C	Surface Area	Heat of Sorption
Pure casein	1.880	35.47	6449	8903
Ca-*g*-AN	1.961	4.64	6728	3826
Ca-*g*-AN-*co*-*n*BMA	2.941	1.89	10,091	1587

mers in casein, especially P*n*BMA, the capillaries are increased to larger diameters[44] when compared to casein. Therefore, the surface area increases with grafting. Grafting of casein with AN reduces the number of polar sites. Therefore, the absorbed moisture level was reduced. Due to the reduction in polar sites, the heat of sorption is also correspondingly reduced due to grafting. The heat of sorption was further reduced by the incorporation of *n*BMA, because of the electronegativities of the methacrylate groups. Smaller values of the heat of sorption suggest that adsorption is of the van der Waals type, since chemisorption is generally accompanied by higher heats of adsorption (20–50 kcal/mol).[45]

The stress–strain behavior of Ca-*g*-AN at different RH levels is presented in Figure 2. It shows that the tensile properties of Ca-*g*-AN are tremendously influenced by the absorbed moisture level. At 17% RH (plot 1 in Fig. 2; low level of moisture), the film shows brittle behavior and the sample breaks before yielding. With increase of the moisture, plasticization takes place, the transition temperature[46] is reduced, and, therefore, the fracture behavior changes from brittle to ductile, showing necking without restabilization with the appearance of a clear-cut yield point. At 73% RH (plot 5 in Fig. 2), there is only a pseudo yield point and the sample cold draws. At 95% RH (plot 6 in Fig. 2), the sample with an absorbed high level of water extends uniformly. In all the above cases, water acts as a plasticizer and brings out an effect similar to the one produced by the temperature.[47,48]

In the case of Ca-*g*-AN-*co*-*n*BMA, due to the incorporation of *n*BMA molecules, the stress–strain curves were moved toward the strain axis when compared to Ca-*g*-AN, even though the level of moisture is almost the same at different RH levels (Fig. 3). Even at 17 RH, the stress–strain curve shows a pseudo yield point and the extension was increased with a reduction in tensile strength due to the incorporation of *n*BMA molecules. The increase in moisture level does not characteristically

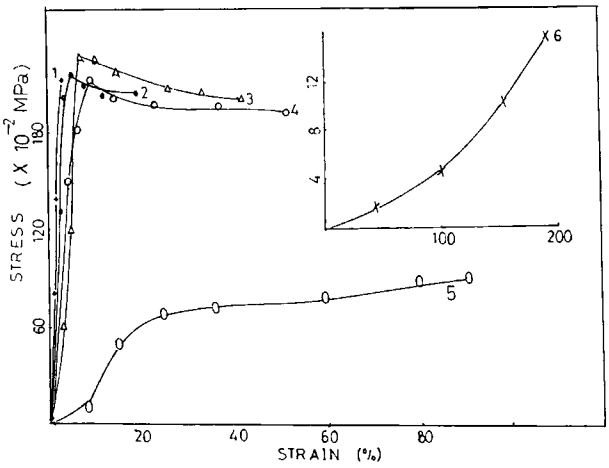

Figure 2 Stress–strain curves of Ca-*g*-AN at various RH levels: (1) 17; (2) 37; (3) 50; (4) 67; (5) 73; (6) 95.

change the stress–strain behavior when compared to Ca-*g*-AN.

The elastic modulus and energy-to-break values obtained for Ca-*g*-AN and Ca-*g*-AN-*co*-*n*BMA are, respectively, presented in Tables III and IV. In the case of Ca-*g*-AN, the elastic modulus considerably decreases with the absorbed moisture level. Above 72% RH, due to the capillary condensation of water, the absorbed moisture level was tremendously increased, which drastically changes the elastic modulus. At low moisture content, the stress and strain at yield point (Table III) was not affected. After 65% RH, tensile parameters change drastically. Due to the addition of P*n*BMA, the stress–strain behavior changes and only pseudo yielding is shown by the samples. The fracture toughness also characteris-

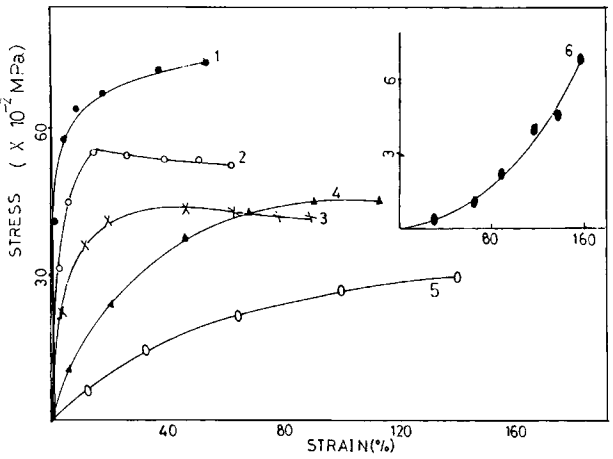

Figure 3 Stress–strain characteristics of Ca-*g*-AN-*co*-*n*BMA films at different RH levels: (1) 17; (2) 37; (3) 50; (4) 67; (5) 73; (6) 95.

Table III Tensile Properties of Ca-*g*-AN at Different RH

RH	Tensile Strength (MPa)	Elongation at Break (%)	Energy to Break (MJ m^{-3})	Elastic Modulus (MPa)	σ_y/σ_b	$\varepsilon_y/\varepsilon_b$
17	221.0 ± 9.4	3.5 ± 0.4	0.69	6900	—	—
37	207.0 ± 13.0	19.5 ± 2.5	3.21	4400	1.05	0.31
50	200.0 ± 9.7	42.3 ± 3.2	7.53	2800	1.13	0.22
67	193.2 ± 12.6	51.4 ± 7.2	9.11	3000	1.12	0.18
72	89.1 ± 14.5	91.3 ± 10.0	5.84	100	0.77	0.27
95	15.5 ± 2.4	194.0 ± 13.0	1.09	6	0.28	0.53

tically changes after 65% RH, where the capillary condensation of water is taking place in the film as mentioned earlier. The ratio of stress and strain at the yield point to the break point (σ_y/σ_b and $\varepsilon_y/\varepsilon_b$) are presented in Table III (Ca-*g*-AN). In general, when σ_y/σ_b is 1, then the material fracture is by a necking (micro)-rupture. Table III suggests that in the case of Ca-*g*-AN, with up to 65% RH, the material fails by necking without restabilization. Similarly, ϵ_y/ϵ_b decreases with RH up to 65% RH and then increases. The absorbed moisture lengthens the neck formed (cold drawing) before break. After 65% RH, necking and cold drawing is very much pronounced and the material flows. Therefore, ϵ_y/ϵ_b shows increased values.

The relationship between the tensile strength and elongation at break with an absorbed level of moisture is presented, respectively, in Figures 4 and 5 for Ca-*g*-AN and Ca-*g*-AN-*co*-*n*BMA. In both cases, the tensile strength values are reduced and elongation at break increased as moisture content increased. In both grafted systems, the effect takes place in three levels. Initially, it was not very much pronounced at the water monolayer formation level and the rate increased at the multilayer formation level. The change in tensile properties is very much pronounced after 65% RH, where the capillary condensation of water molecules is taking place.

The rate of change of the tensile property with the change of absorbed moisture (dy/dx in Figs. 4 and 5) shows that in the case of Ca-*g*-AN-*co*-*n*BMA the effect was very much pronounced below the 10% absorbed moisture level, whereas in the case of Ca-*g*-AN, the change in tensile property with the change in absorbed moisture is not very much changed up to 65% RH. These relationships clearly show that the effect produced by water is totally different in both Ca-*g*-AN and Ca-*g*-AN-*co*-*n*BMA, even though the films absorb a comparable level of moisture.

Biaxial Testing

Stress–strain characteristics under various levels of applied lateral stress in the longitudinal direction are presented in Figures 6 and 7, respectively, for Ca-*g*-AN and Ca-*g*-AN-*co*-*n*BMA. The stress–strain curve of uniaxially tested grafted casein films is also presented for comparison.

Figure 6 shows that the type of yielding is of the necking type. Initially, the stress rapidly increases with increase of the strain, and after the yield point, necking takes place. After the yield point, the stress decreases with the strain. Due to the application of lateral stress, the stress–strain behavior was not very much changed. In the case of Ca-*g*-AN-*co*-*n*BMA, the stress increases with strain with a pseudo yield point. Even though the stress–strain behavior was not much influenced by the application of lateral stress, both tensile strength and elongation at break were considerably reduced and the behavior is more

Table IV Tensile Properties of Ca-*g*-AN-*co*-*n*BMA at Different RH

RH	Tensile Strength (MPa)	Elongation at Break (%)	Energy to Break (MJ m^{-3})	Elastic Modulus (MPa)
17	74.0 ± 6.0	52.8 ± 6.2	3.44	4115
37	52.5 ± 4.3	61.4 ± 2.9	3.06	1000
50	42.6 ± 2.7	88.9 ± 6.9	3.53	938
67	45.6 ± 3.2	113.0 ± 7.8	3.84	200
73	30.3 ± 1.9	141.0 ± 2.9	2.80	50
95	7.0 ± 0.6	160.0 ± 1.9	0.35	6

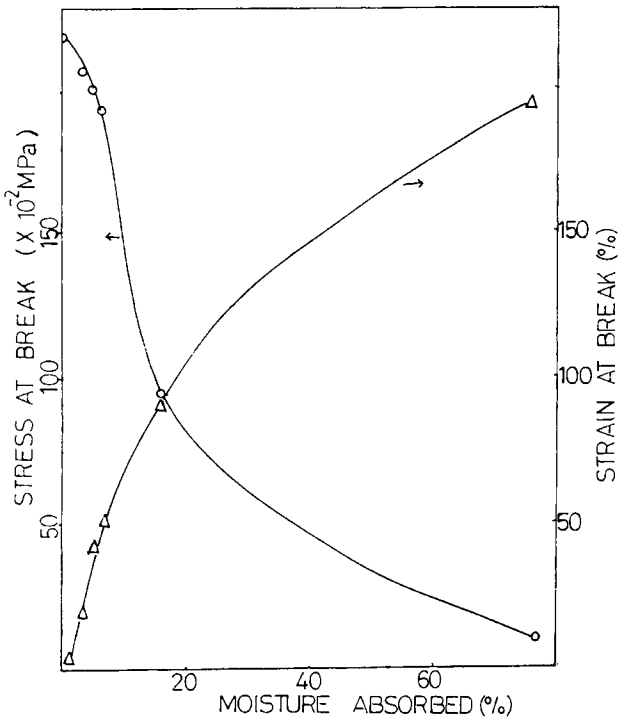

Figure 4 Effect of absorbed moisture level on stress and strain at break (Ca-*g*-AN).

toward the brittle type of fracture. With increase of lateral stress, the flow region in the stress–strain curve was affected.

The effect of applied lateral stress on the tensile strength and elongation at break are presented in Figure 8. Due to the application of stress in the lateral direction, the tensile strength in the longitudinal direction was very much affected. The stress value suddenly decreases, and after a definite value, the effect levels off with increase of the lateral stress. The reduction in tensile strength due to the lateral stress application was 28%, whereas it is only 82.3% in the case of elongation at break (Ca-*g*-AN). Stress–strain curves show that although the overall pattern was not affected the cold-drawing region was affected due to the application of lateral stress.

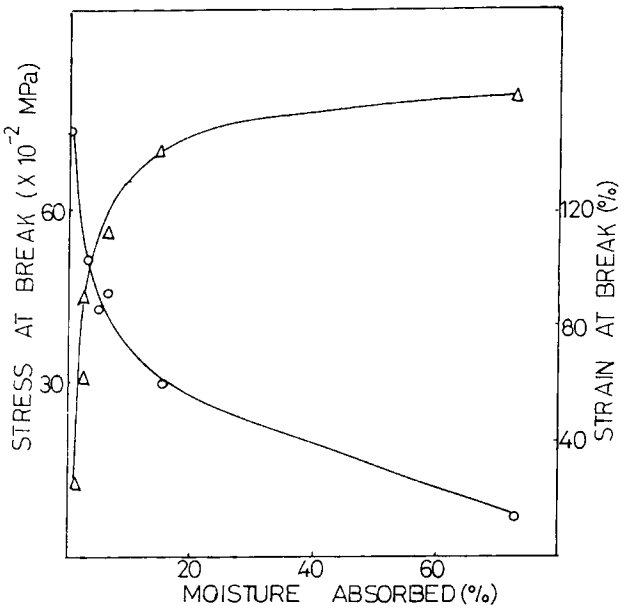

Figure 5 Effect of absorbed moisture level on stress and strain at break (Ca-*g*-AN-*co*-*n*BMA).

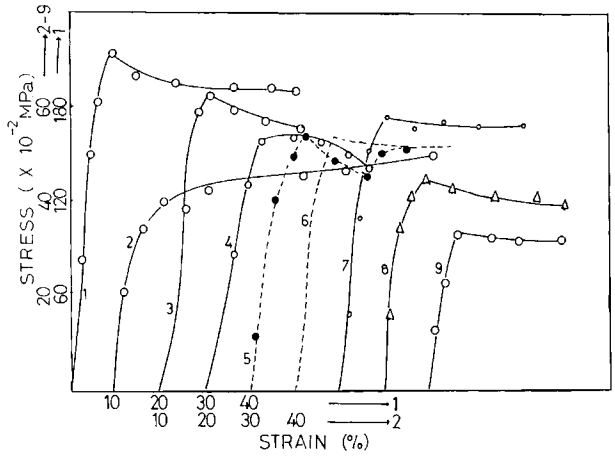

Figure 6 Stress–strain curves of Ca-*g*-AN under various applied lateral stresses: (1) uniaxial; (2) 2.5; (3) 5; (4) 10; (5) 20; (6) 30; (7) 40; (8) 50; (9) 65.

The effect of applied lateral stress on tensile properties in the longitudinal axis for Ca-*g*-AN-*co*-*n*BMA is presented in Figure 9. The tensile strength initially shows a steep decrease and shows practically no change beyond a lateral stress of 5×10^{-2} MPa.

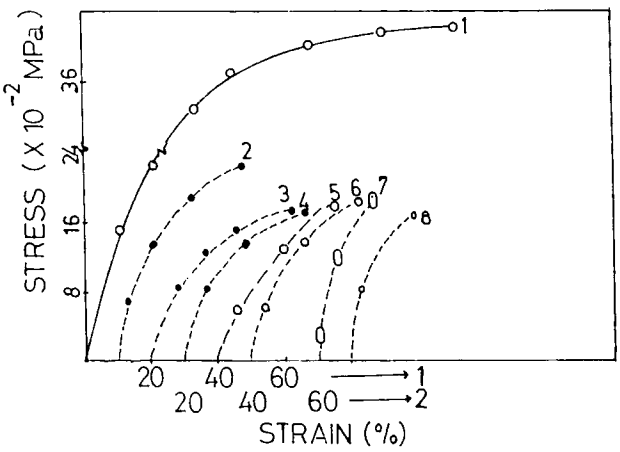

Figure 7 Stress–strain curves of Ca-*g*-AN-*co*-*n*BMA under various applied lateral stresses: (1) uniaxial; (2) 2.5; (3) 5.0; (4) 10.0; (5) 20; (6) 30.0; (7) 40.0; (8) 45.0.

Tensile strength and elongation at break in the longitudinal direction was reduced to 36.4% and 32.3%, respectively, of the original value. Comparison of the results of both systems reveal that due to the incorporation of *n*BMA the response of tensile strength in the longitudinal direction is changed and shows more response in the case of elongation at break, since the rigidity of the polymer is affected due to the presence of flexible *n*BMA chains.

CONCLUSIONS

Studies on the effect of relative humidity and lateral stress clearly show the mechanical response of the grafted casein films under a simulated application condition. Variation of the relative humidity affects the tensile properties in three stages, depending on the level of absorption of water. Applied lateral stress arrests lateral contraction in casein films and reduces tensile strength and elongation at break in the longitudinal direction. In the case of tough films, the decrease in elongation at break is not very much pronounced (Ca-*g*-AN) when compared to films having more flexibility. These studies give a true picture of the properties under different application conditions.

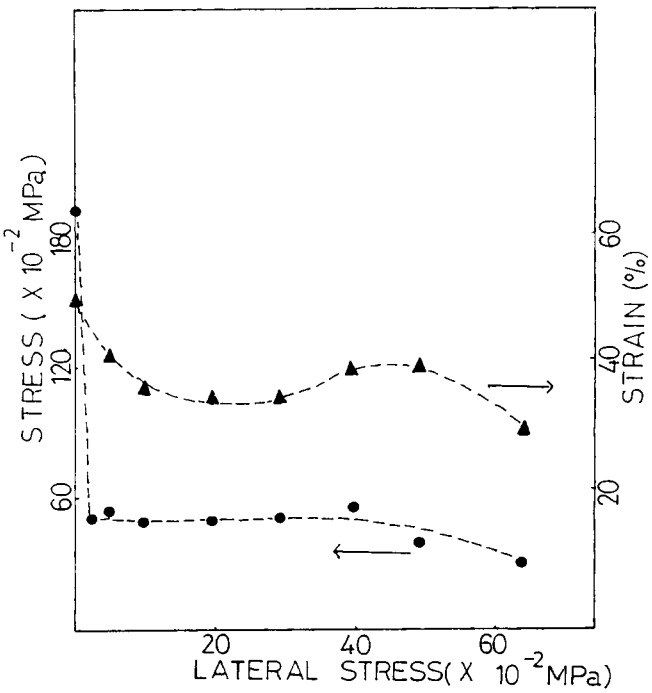

Figure 8 Effect of applied lateral stress on stress and strain at break (Ca-*g*-AN).

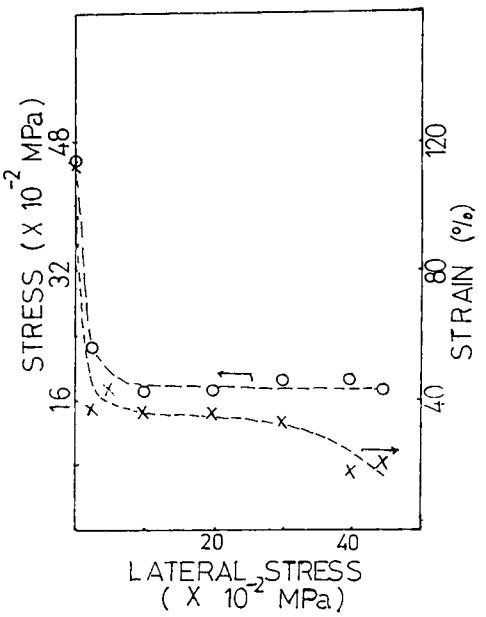

Figure 9 Effect of applied lateral stress on stress and strain at break (Ca-*g*-AN-*co*-*n*BMA).

REFERENCES

1. D. Satyanarayana and P. R. Chatterji, *J. Macromol. Sci. Pure Appl. Chem. A*, **29,** 625 (1992).
2. J. Stejski, D. Strakova, and P. Kratochvil, *J. Appl. Polym. Sci.*, **36,** 215 (1988).
3. J. S. Sukla, S. C. Tiwari, and C. K. Sharma, *J. Appl. Polym. Sci.*, **34,** 191 (1987).
4. J. S. Sukla and S. C. Tiwari, *J. Appl. Polym. Sci.*, **38,** 291 (1989).
5. N. Y. Abou-Zeid, A. Kigazy, and A. Hebeish, *Angew. Macromol. Chem.*, **121,** 69 (1984).
6. A. Bazuaye, F. E. Okieimen, and O. B. Said, *J. Polym. Sci. Polym. Lett. Ed.*, **27,** 433 (1989).
7. D. Mohan, G. Radhakrishnan, S. Rajadurai, K. Venkata Rao, and G. G. Cameron, *J. Polym. Sci. Polym. Chem. Ed.*, **27,** 2123 (1989).
8. D. Mohan, G. Radhakrishnan, and S. Rajadurai, *Leather Sci.*, **32,** 134 (1985).
9. D. Mohan, G. Radhakrishnan, and S. Rajadurai, *J. Macromol. Sci. Chem. A*, **22,** 75 (1985).
10. X. Jinyu, and L. Ning, *Xibei Qinggongye Xueyuan Xuebao*, 1986 (3) 34-9; *Chem. Abstr.* **110,** 8751f (1986).
11. D. Mohan, PhD Thesis, University of Madras, 1983.
12. I. M. Ward, *Mechanical Properties of Solid Polymer*, 2nd ed., Wiley-Interscience, New York, 1983.
13. A. D. Jenkins, Ed., *Polymer Science*, North-Holland, London, 1972, Vol. 1, Chap. 8.
14. B. Golding, *Polymers and Resins*, Van Nostrand, New York, 1959.
15. K. Nakagawa, Y. Konaka, and Y. Sato, *Polym. Prep. Jpn.*, **26,** 392 (1977).

16. E. Ito and Y. Kobayashi, *J. Appl. Polym. Sci.*, **22,** 1143 (1978).
17. J. M. Barton and D. C. L. Grenfield, *Br. Polym. J.*, **18,** 51 (1986).
18. A. Apicella and L. Nicolais, in *Epoxy Resins and Composites,* I. K. Dusek, Ed., Advances in Polymer Science Vol. 72, Springer-Verlag, Berlin, 1985, p. 69.
19. F. Yang, R. D. Gilbert, R. E. Fornes, and J. D. F. Memory, *J. Polym. Sci. Polym. Chem. Ed.*, **24,** 2609 (1986).
20. J. A. Barrie, H. Rudd, and P. S. Sagoo, *Br. Polym. J.*, **18,** 303 (1986).
21. E. Ito and Y. Kobayashi, *J. Appl. Polym. Sci.*, **25,** 2145 (1980).
22. R. J. Gardner and J. R. Martin, *J. Appl. Polym. Sci.*, **25,** 2353 (1980).
23. T. S. Ellis, *J. Appl. Polym. Sci.*, **36,** 451 (1988).
24. H. K. Reimschuessel, *J. Polym. Sci. Polym. Chem. Ed.*, **16,** 1229 (1978).
25. A. D. Jenkins, Ed., *Polymer Science,* North-Holland, London, 1972.
26. N. Somanathan, R. Usha, and R. Sanjeevi, *Leather Sci.*, **33**(10), 281 (1986).
27. H. Tanaka, K. Kurihara, M. Morita, K. Mori, and S. Okajima, *J. Polym. Sci. Part B,* **9,** 723 (1971).
28. I. K. Hopkins, W. O. Baker, and J. B. Howard, *J. Appl. Phys.*, **21,** 206 (1950).
29. B. B. S. T. Boonstra, *J. Appl. Phys.*, **21,** 1098 (1950).
30. C. C. Hsiao and J. A. Sauer, *J. Appl. Phys.*, **21,** 1071 (1950).
31. H. Tanaka, K. Kurihara, M. Morita, K. Mori, and S. Okajima, *J. Polym. Sci. Polym. Lett. Ed.*, **9,** 723 (1971).
32. N. Iwato, H. Tanaka, and S. Okajima, *J. Appl. Polym. Sci.*, **19,** 303 (1975).
33. K. Matsumoto, J. F. Fellers, and J. L. White, *J. Appl. Polym. Sci.*, **26,** 85 (1981).
34. J. Y. Guan, R. F. Saraf, and R. S. Porter, *J. Appl. Polym. Sci.*, **33,** 1517 (1987).
35. P. P. Purslow, A. Bigi, M. A. Ripamonti, and N. Roveri, *Int. J. Biol. Macromol.*, **6,** 21 (1984).
36. J. M. Hawthorne, *J. Appl. Polym. Sci.*, **26,** 3317 (1981).
37. N. Somanathan, C. Rami Reddy, N. Radhakrishnan, and R. Sanjeevi, *Eur. Polym. J.*, **23,** 489 (1987).
38. *International Critical Tables of Numerical Data, Physics, Chemistry and Technology,* Vol. 1, National Research Council, McGraw-Hill, New York, 1926.
39. N. Somanathan, V. Arumugam, R. Sanjeevi, and V. Narashimhan, *J. Appl. Polym. Sci.*, **34,** 2299 (1987).
40. N. Somanathan, M. D. Naresh, V. Arumugam, and R. Sanjeevi, *Polym. J.*, **24,** 603 (1992).
41. S. Kulasekaran, Y. Lakshminarayana, S. Rajadurai, K. T. Joseph, and M. Santappa, *Leather Sci.*, **2c3,** 385 (1976).
42. N. Somanathan, R. Ganesh Jeevan, and R. Sanjeevi, *Polym. J.*, **23**(9), 939 (1993).
43. S. Brunauer, P. H. Emmett, and E. Teller, *J. Am. Chem. Soc.*, **60,** 309 (1938).
44. N. Somanathan, V. Arumugam, R. Sanjeevi, and T. S. Ranganathan, *J. Soc. Leather Trades Chem.*, **71,** 108 (1987).
45. J. R. Kanagy, *J. Am. Leather Chem. Assoc.*, **42,** 98 (1947).
46. N. M. Bikales, Ed., *Mechanical Properties of Polymers—Encyclopedia Reprints,* ed. N. M. Bikales, Ed., Wiley-Interscience, New York, 1971.
47. N. Somanathan, PhD Thesis, University of Madras, 1992.
48. N. Somanathan, *J. Appl. Polym. Sci.*, **52,** 1069 (1994).

Received October 10, 1995
Accepted June 1, 1996